Research Square

Preprints are preliminary reports that have not undergone peer review.
They should not be considered conclusive, used to inform clinical practice,
or referenced by the media as validated information.

Mitochondrial Complex I Inhibition Is Associated with Macrophage Metabolic Reprogramming and Impaired Chronic Diabetic Wound Healing

Zhang Yongxin
Youjiang Medical College for Nationalities
Wang Zenan
Youjiang Medical College for Nationalities
Xiang Yueyu
Youjiang Medical College for Nationalities
Xian Yifan
Youjiang Medical College for Nationalities
Li Guanlin
Youjiang Medical College for Nationalities
Yang Putong
Youjiang Medical College for Nationalities
Sha Yin
Youjiang Medical College for Nationalities
Pan Juexiu
Youjiang Medical College for Nationalities
Li Haijuan
Affiliated Hospital of Youjiang Medical University for Nationalities
Biaoliang Wu
yymucun@mun.edu.cn

Affiliated Hospital of Youjiang Medical University for Nationalities

Research Article

Keywords: chronic diabetic wounds, macrophage metabolic reprogramming, macrophage polarization, mitochondrial complex I inhibition, glycolysis

Posted Date: November 11th, 2026

DOI: https://doi.org/10.21203/rs.3.rs-11259098/v1

License: This work is licensed under a Creative Commons Attribution 4.0 International License.
Read Full License

Additional Declarations: No competing interests reported.

Mitochondrial Complex I Inhibition Is Associated with Macrophage Metabolic Reprogramming and Impaired Chronic Diabetic Wound Healing

Yongxin Zhang[1,2,3,4]
Zenan Wang[1,2,3,4]
Yueyu Xiang [1,2,3,4]
Yifan Xian[1,2,3,4]
Guanlin Li[1,2,3,4]
Putong Yang[1,2,3,4]
Yin Sha[1,2,3,4]
Juexiu Pan[1,2,3,4]
Haijuan Li[2,3,4]
Biaoliang Wu[2,3,4]
1 School of Clinical Medicine, Youjiang Medical University for Nationalities, Baise 533000, Guangxi, China
2 Department of Endocrinology, The Affiliated Hospital of Youjiang Medical University for Nationalities, Baise 533000, Guangxi, China
3 Key Laboratory of Medical Research Basic Guarantee for Immune-Related Diseases Research of Guangxi (Cultivation), Youjiang Medical University for Nationalities, Baise 533000, Guangxi, China
4 Baise Key Laboratory of Metabolic Diseases, Baise 533000, Guangxi, China

Corresponding Author: Biaoliang Wu, Email: yymucun@mun.edu.cn

Abstract

Aim

To investigate the association of macrophage metabolic reprogramming with wound healing and angiogenesis in a murine model of chronic diabetic wounds.

Methods

Diabetes was induced in mice using a high-fat diet combined with streptozotocin (STZ). Successful induction was defined as a fasting blood glucose level ≥16.7 mmol/L on two separate days. Mice were randomly allocated to normal control, diabetic, vehicle, and rotenone groups. A full-thickness excisional wound approximately 2 cm in diameter was created on the dorsum of each mouse. The

rotenone group received daily intraperitoneal rotenone (1 mg/kg), whereas the vehicle group received an equivalent volume of vehicle; the normal control and diabetic groups received no additional treatment. Wound closure was evaluated on days 4, 8, 12, and 16. Histological changes were assessed by hematoxylin and eosin staining; LDHA, PKM2, and CS expression by immunohistochemistry; and iNOS and Arg-1 mRNA expression by RT-qPCR.

Results

Compared with the normal control group, the diabetic, vehicle, and rotenone groups showed delayed wound closure. On days 8, 12, and 16, wound closure rates were lower in all three groups than in normal controls, with the rotenone group showing the lowest rates at each time point. Histological examination further revealed greater inflammatory cell infiltration and delayed re-epithelialization in the rotenone group. In this group, LDHA and PKM2 expression began to increase on day 8. Relative to normal controls, LDHA expression was significantly higher on days 8 and 16, PKM2 expression was significantly higher on days 8, 12, and 16, and CS expression was lower at all assessed time points. In addition, iNOS mRNA expression was increased on days 4, 8, and 12, whereas Arg-1 mRNA expression was decreased on days 4 and 8 but increased on day 12.

Conclusions

Rotenone further delayed chronic wound healing in diabetic mice, accompanied by changes consistent with enhanced glycolysis, impaired oxidative metabolism, and an imbalance between M1- and M2-associated macrophage phenotypes. These findings suggest that macrophage metabolic reprogramming may contribute to impaired repair of chronic diabetic wounds and may represent a potential target for future intervention.

Keywords: chronic diabetic wounds; macrophage metabolic reprogramming; macrophage polarization;

mitochondrial complex I inhibition; glycolysis

1. Introduction

Diabetes mellitus(DM) is a chronic metabolic disorder characterized by persistent hyperglycemia resulting from impaired insulin secretion, insulin action, or both[1]. According to the International Diabetes Federation, approximately 589 million adults worldwide were living with diabetes in 2024, the vast majority of whom had type 2 diabetes mellitus (T2DM); this number is projected to continue rising in the coming years[2,3]. Chronic diabetic wounds, particularly diabetic foot ulcers (DFUs), are a major cause of disability among individuals with diabetes because of their delayed healing, high recurrence rates, and substantial risk of amputation[4,5]. Despite recent advances in wound management, chronic diabetic wounds are often characterized by persistent inflammation and impaired tissue repair. However, the molecular mechanisms underlying their development and progression remain incompletely understood, highlighting the importance of identifying key regulatory processes that influence wound healing.

Macrophages are key immunoregulatory cells in wound

inflammation and repair. During normal healing, they gradually shift from an early proinflammatory M1 state to a later reparative M2 state. In diabetes, hyperglycemia, oxidative stress, and persistent inflammation disrupt this transition. Consequently, M1 activation persists, whereas M2 function is impaired. These changes may prolong inflammation and delay wound healing[4,5]. Restoring macrophage functional homeostasis may therefore represent a potential approach to improving chronic diabetic wound healing.

Recent studies in immunometabolism suggest that macrophage function is regulated not only by

77 inflammatory signals but also by cellular metabolic states. M1 macrophages are generally considered to
78 rely predominantly on glycolysis, whereas M2 macrophages depend more heavily on mitochondrial
79 oxidative phosphorylation(OXPHOS) to support their reparative functions. Glycolysis-related
80 molecules, including lactate dehydrogenase A(LDHA) and pyruvate kinase M2(PKM2), together with
81 citrate synthase(CS), a key enzyme in the tricarboxylic acid cycle, are involved in macrophage
82 metabolic regulation[6-9]. Although diabetes is associated with mitochondrial dysfunction and
83 metabolic abnormalities, it remains unclear whether impaired mitochondrial OXPHOS promotes
84 macrophage metabolic reprogramming and subsequently affects macrophage polarization and chronic
85 diabetic wound healing.

86 Rotenone is a well-established inhibitor of mitochondrial complex I that suppresses oxidative
87 phosphorylation, promotes a metabolic shift toward glycolysis, and increases reactive oxygen species
88 production[10]. In this study, a murine model of chronic diabetic wounds was established, and rotenone
89 was used to inhibit mitochondrial complex I. Changes in markers related to glucose metabolic
90 reprogramming, macrophage polarization, and wound healing were evaluated to explore the potential
91 involvement of mitochondrial dysfunction-associated macrophage metabolic reprogramming in chronic
92 diabetic wound repair and to provide experimental evidence for further investigation of the underlying
93 immunometabolic mechanisms.

94

95 **2 Materials and Methods**

96 **2.1 Animals**

97 A total of 128 six-week-old male specific pathogen-free C57BL/6J mice (20 ± 2 g) were obtained from

Changsha Tianqin Biotechnology Co., Ltd. [animal production license No. SCXK (Xiang) 2024-0021]. All animal procedures were approved by the Ethics Committee of Youjiang Medical University for Nationalities (approval Nos. 2024092503 and 2025040200).

2.2 Reagents and Equipment

The principal reagents included streptozotocin (STZ; Beijing Solarbio Science & Technology Co., Ltd.; Cat. No. S8050-1g), rotenone (GLPBIO; Cat. No. 83794), tribromoethanol (Nanjing Aibei Biotechnology Co., Ltd.; Cat. No. M2920), and a reverse transcription kit (Yugong Biolabs; Cat. No. EG151133S). Antibodies against Arg-1 (Proteintech; Cat. No. 66129-1-Ig), iNOS (Jiangsu Qinke Biotechnology Research Center Co., Ltd.; Cat. No. 22226-1-AP), LDHA (Proteintech; Cat. No. 14546-1-AP), PKM2 (Proteintech; Cat. No. 15822-1-AP), CS (Proteintech; Cat. No. 16131-1-AP), and CD31 (Affinity Biosciences; Cat. No. BF8133) were also used.

The principal instruments included a gradient thermal cycler (Bio-Rad Laboratories, USA), a real-time quantitative PCR system (Roche), a UV spectrophotometer (Implen, Germany), a Multiskan microplate reader (Labsystems, Finland), and an upright fluorescence microscope (Nikon, Japan).

2.3 Methods

2.3.1 Establishment and Grouping of the Murine Chronic Diabetic Wound Model

Following the protocol described by Dong[11], mice were acclimatized for 1 week and randomly assigned to the normal control, diabetic model, rotenone, and vehicle groups (n = 32 per group). The normal control group remained on a standard diet, whereas the other three groups received a high-fat diet for 4 weeks. After a 12-h fast with free access to water, these mice were intraperitoneally injected

with STZ (50 mg/kg/day) for 5 consecutive days, while the normal control group received an equal volume of citrate buffer. One week after model induction, mice with fasting blood glucose (FBG) levels ≥16.7 mmol/L on two consecutive measurements were considered diabetic. Mice that did not meet this criterion received one additional injection of STZ at the same dose.

One week after successful establishment of the diabetic model, the mice were anesthetized by intraperitoneal administration of 1.25% tribromoethanol (0.2 mL/10 g). Adequate anesthetic depth was confirmed by the absence of a response to toe-pinch stimulation. And a circular full-thickness skin wound approximately 2 cm in diameter was created on the dorsum. The normal control and diabetic model groups received standard sterile gauze dressings. The rotenone group received a daily intraperitoneal injection of rotenone (1 mg/kg), whereas the vehicle group received an equal volume of vehicle. All interventions continued until the designated observation endpoint. The rotenone dose of 1 mg/kg was selected based on preliminary experiments, in which this dose produced a measurable biological effect without causing overt toxicity or excessive mortality.

2.3.2 Sample Collection

The day of wound creation was defined as day 0. Wounds were photographed on days 0, 4, 8, 12, and 16 to document healing. The mice were anesthetized as described above. Adequate anesthetic depth was confirmed by the absence of a response to toe-pinch stimulation. Full-thickness tissue samples, including the wound and approximately 0.5 cm of surrounding tissue, were then collected. Each sample was divided into two portions. One portion was snap-frozen in liquid nitrogen and stored at −80 °C for reverse transcription quantitative PCR (RT-qPCR). The other portion was fixed in 4% paraformaldehyde and embedded in paraffin for hematoxylin and eosin (H&E) staining and immunohistochemistry. After tissue collection, anesthetic depth was reconfirmed by the absence of a

response to toe-pinch stimulation. The mice were then euthanized by cervical dislocation. Death was confirmed by the permanent cessation of respiration and heartbeat.

2.3.3 Histological Assessment of Wound Tissue by Hematoxylin and Eosin Staining

Tissue samples were fixed in 4% paraformaldehyde at room temperature for 24–48 h. They were then dehydrated through a graded ethanol series and embedded in paraffin. The paraffin blocks were cut into 3 μm sections. After deparaffinization and rehydration, the sections were stained with hematoxylin and eosin (H&E). Finally, the sections were dehydrated, mounted, and examined under a light microscope to assess tissue architecture, inflammatory cell infiltration, and granulation tissue formation.

2.3.4 Immunohistochemical Detection of Metabolism- and Macrophage Polarization-Related Markers

After deparaffinization and rehydration, the sections underwent antigen retrieval, endogenous peroxidase blocking with hydrogen peroxide, and serum blocking. They were then incubated overnight at 4 °C with primary antibodies against LDHA, PKM2, and CS (all diluted 1:200), followed by horseradish peroxidase (HRP)-conjugated secondary antibodies. Immunoreactivity was visualized with 3,3′-diaminobenzidine (DAB), followed by hematoxylin counterstaining, dehydration, and mounting. Immunostaining intensity was quantified using ImageJ software.

2.3.5 RT-qPCR Analysis of Nos2 and Arg1 mRNA Expression

Total RNA was extracted using TRIzol reagent (50 mg per 1 mL). After assessing RNA concentration and purity, the RNA was reverse-transcribed into cDNA. RT-qPCR was performed using SYBR Green to quantify Nos2 and Arg1 mRNA expression, with Actb (β-actin) as the reference gene. Relative

expression was calculated using the 2^−ΔΔCt method. The primers were designed and synthesized by Sangon Biotech (Shanghai) Co., Ltd., and their sequences are listed in Table 1.

Table 1 Primer sequences for genes related to RT-qPCR experiment on mouse wound

Primer name	Sequence（5' to 3'）
iNOS-F	GACGCTCGGAACTGTAGCAC
iNOS-R	TCATGTTTGCCGTCACTCCG
Arg-1-F	TGGGCAACCTGTGTCCTTTC
Arg-1-R	AGGGTCTACGTCTCGCAAGC
β-actin-F	ACTGCCGCATCCTCTTCT
β-actin-R	TCAACGTCACACTTCATGATGGA

2.3.6 Statistical Analysis

Statistical analyses were performed using IBM SPSS Statistics version 27.0 and GraphPad Prism version 9.5.1. Continuous variables were tested for normality using the Shapiro–Wilk test. Normally distributed continuous data are presented as the mean ± standard deviation (x ± S). Non-normally distributed data are presented as the median and interquartile range. Differences among groups were assessed using one-way ANOVA. Repeated measures ANOVA was used for data collected over time. Post hoc multiple comparisons were adjusted using the Bonferroni correction. $p< 0.05$ was considered statistically significant.

3 Results

3.1 Diabetic Mice Exhibited Changes in General Condition

Compared with the normal control group, diabetic mice exhibited typical diabetic manifestations, including polydipsia, polyuria, polyphagia, and weight loss. Daily water intake increased to 20–50 mL, and the bedding became damp and malodorous. The mice also appeared less alert, showed slower responses and reduced spontaneous activity, and developed dry, dull, and ruffled fur.

3.2 Compared with the Normal Control Group, Rotenone Delayed Inflammation Resolution, Granulation Tissue Formation, and Re-epithelialization in Diabetic Wounds and Reduced Wound Closure Rate ($P < 0.05$)

Gross observation and H&E staining revealed differences in wound healing among the groups (Fig.1A and 1B). On day 4, all wounds were in the inflammatory phase, with more pronounced inflammation in the diabetic and rotenone groups than in the normal control group. Thereafter, inflammation gradually subsided in the normal control group, accompanied by granulation tissue formation and re-epithelialization. Repair was delayed in the diabetic and vehicle groups, while the rotenone group showed more persistent inflammation and less granulation tissue formation and re-epithelialization, with delayed repair remaining evident on day 16. Wound closure was slower in the other three groups than in the normal control group. On day 4, closure rates were lower in the diabetic and rotenone groups than in the normal control group ($p < 0.05$). Significant differences among the groups were observed on days 8, 12, and 16 ($p < 0.001$), with the rotenone group maintaining a comparatively low closure rate throughout the observation period (Fig. 1C).

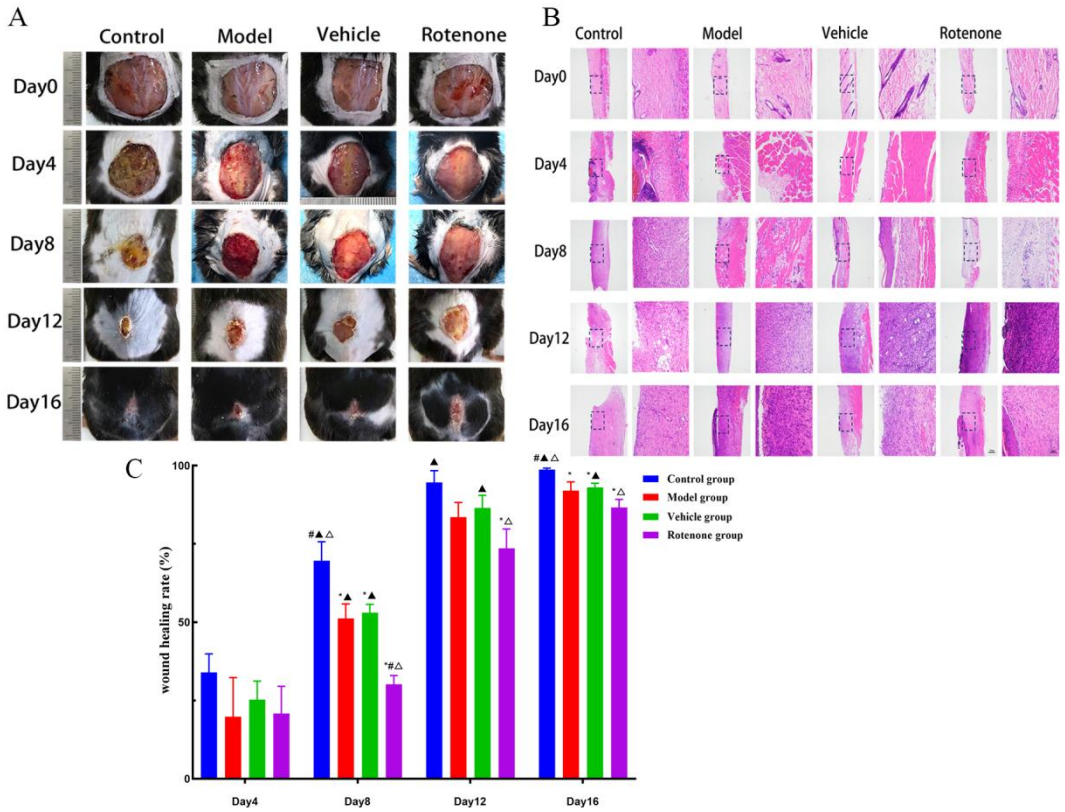


Figure 1 Comparison of wound healing among groups at different time points A: Comparison of wound healing; B: H&E staining of the wound (Scale bar = 50 μm，200 μm) ; C: Comparison of wound healing rates（n=6, $\bar{x}$±S; %）

3.3 Changes in Glucose Metabolism Markers After Rotenone Treatment in Diabetic Mouse Wounds

Immunohistochemical analysis revealed distinct expression patterns of LDHA, CS, and PKM2 among the groups.

LDHA expression was higher in the rotenone group than in the normal control group on days 8 and 16 ($P < 0.05$). No significant difference was observed among the groups on days 4 and 12 ($p > 0.05$) (Fig. 2A and 2D).

CS expression showed an overall downward trend from day 4 onwards. Compared with the normal control group, the rotenone group exhibited lower CS expression on days 4, 8, 12, and 16 ($p < 0.05$),and has the lowest levels among the groups at most time points(Fig. 2A and 2E).

PKM2 expression was higher in the rotenone group than in the normal control group ($p < 0.05$) and remained relatively high at the later time points. However, no significant between-group difference in PKM2 expression was observed on day 4 ($p > 0.05$) (Fig. 2D and 2F).

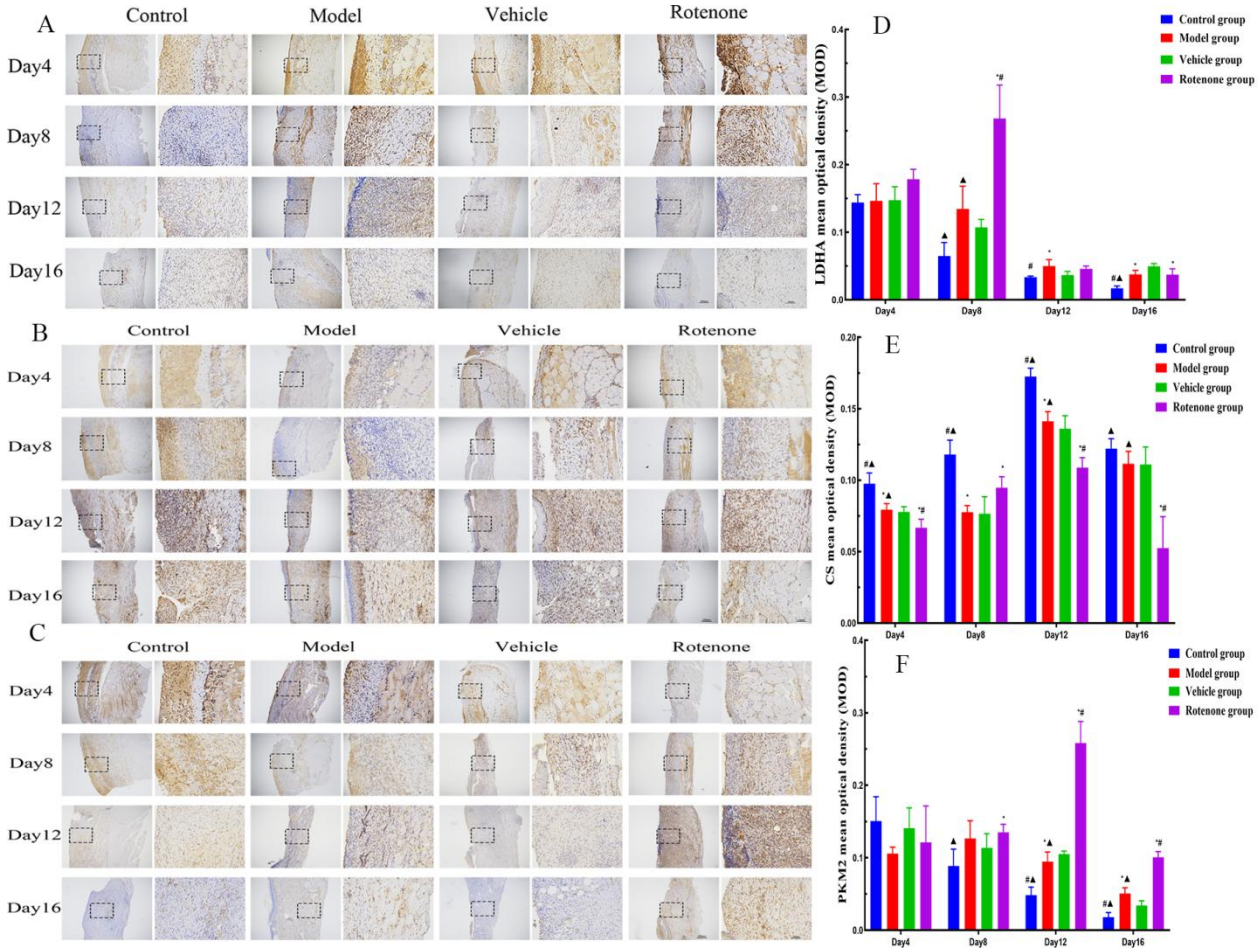


Figure 2 Mean optical density analysis of LDHA, CS, and PKM2 expression A: Immunohistochemical staining of LDHA protein expression in wound tissue (Scale bar = 50 μm, 200 μm); B: Immunohistochemical staining of CS protein expression in wound tissue (Scale bar = 50 μm，200 μm); C: Immunohistochemical staining of PKM2 protein expression in wound tissue (Scale bar = 50 μm，200 μm); D: LDHA protein expression in wound tissue (x̄±S); E: CS protein expression in wound tissue (x̄±S); F: PKM2 protein expression in wound tissue (x̄±S)

3.4 Changes in Macrophage Polarization Markers After Rotenone Treatment in Diabetic Wounds in Mice

RT qPCR analysis showed dynamic changes in iNOS and Arg-1 mRNA expression among the groups during wound healing.

iNOS mRNA expression differed significantly among the groups on days 4, 8, and 12 ($p < 0.001$) and was higher in the rotenone group than in the normal control group ($p < 0.05$). However, the difference between these two groups was no longer significant on day 16 (Fig. 3B).

Arg-1 mRNA expression also differed significantly among the groups on days 4, 8, and 12. Compared with the normal control group, the rotenone group showed lower Arg-1 mRNA expression on days 4 and 8 ($p < 0.05$), but higher expression on day 12 ($p < 0.05$). No significant difference was observed among the groups on day 16 (Fig. 3C).

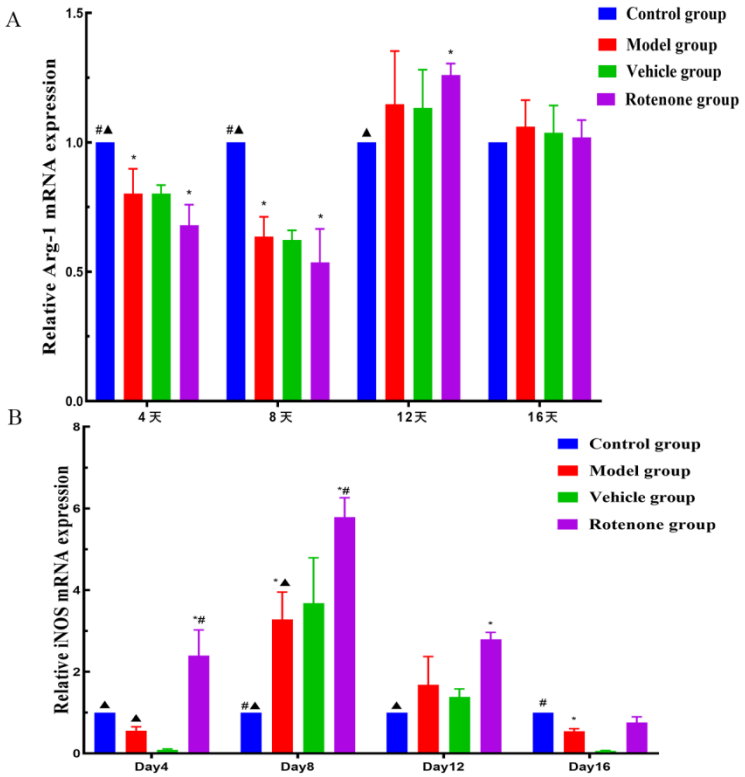


Figure 3 Relative expression of Arg-1 mRNA and iNOS mRNA A: Comparison of Arg-1 mRNA expression levels in wound tissues of mice in each group（n=5, $\bar{x} \pm S$）
B: Comparison of iNOS mRNA expression levels in wound tissues of mice in each group（n=4, $\bar{x} \pm S$）

4 Discussion

We established a murine model of chronic diabetic wounds and administered rotenone, a mitochondrial

complex I inhibitor. This study explored the potential relationships among mitochondrial dysfunction, macrophage metabolic reprogramming, and impaired wound healing. Rotenone treatment delayed wound healing. Such change was accompanied by increased expression of iNOS, LDHA, and PKM2 and decreased expression of CS. These findings suggest that mitochondrial dysfunction may be associated with a proinflammatory macrophage phenotype, enhanced glycolysis, and reduced oxidative metabolism. These changes may contribute to impaired healing of chronic diabetic wounds. However, no cell-specific metabolic intervention was performed. Therefore, these associations cannot be interpreted as direct causal relationships.

The transition of macrophages from an early proinflammatory state to a later reparative state is important for normal wound healing. Louiselle et al. reported that this transition is disrupted in diabetic wounds, with persistent proinflammatory activity and impaired reparative function[12]. In the present study, iNOS expression increased at early time points in the rotenone group, whereas changes in LDHA and PKM2 were most evident from days 8 to 12. This temporal pattern suggests that inflammatory phenotypic changes and metabolic reprogramming may not occur simultaneously. It is broadly aligns with the preferential reliance of M1-associated macrophages on glycolysis and of M2-associated macrophages on oxidative phosphorylation[13,14]. The temporal sequence and regulatory links between these processes remain unclear. Arg-1 expression did not fully parallel iNOS expression. Arg-1 is associated with cell proliferation, collagen synthesis, and tissue repair[15]. This discrepancy suggests that M2- associated markers may not fully reflect reparative function in the context of diabetes and mitochondrial dysfunction. Accordingly, combining M1 and M2 markers with functional measures may provide a more comprehensive assessment of macrophage function in diabetic wounds.

Consistent with the molecular findings, wound closure was reduced in the diabetic and rotenone-treated groups from day 8 onward. The rotenone-treated group showed a more pronounced delay at several time points, accompanied by persistent inflammatory infiltration and impaired re-epithelialization. Beyond energy metabolism, mitochondria also regulate oxidative stress and inflammation, and macrophage mitochondrial metabolism changes across different stages of wound repair[16,17]. Diabetes-associated hyperglycemia and oxidative stress may compromise this metabolic adaptation. Thus, rotenone-mediated complex I inhibition may exacerbate local metabolic dysregulation; aithough whether it impairs repair primarily by disrupting stage-dependent macrophage metabolism remains uncertain.

The metabolic profile further supported a possible shift toward glycolysis. The rotenone group showed increased LDHA and PKM2 expression but persistently lower CS expression. This profile may reflect enhanced glycolysis and reduced oxidative metabolism after complex I inhibition. It is broadly consistent with the metabolic characteristics of M1 macrophages[14]. PKM2 expression also generally paralleled iNOS expression. However, the ratio of PKM2 dimers to tetramers and its nuclear translocation were not assessed. Its role in inflammatory regulation therefore remains unclear. These results suggest a possible link between metabolic changes and the inflammatory phenotype. The underlying mechanisms require further investigation.

Overall, our findings suggest that mitochondrial dysfunction may be associated with macrophage metabolic reprogramming and persistent proinflammatory activity. These changes may contribute to impaired healing of chronic diabetic wounds. Future studies could integrate metabolic interventions targeting specific cell types, multiomics analyses, and lineage tracing. These approaches may help clarify the cellular and temporal mechanisms involved.

Author Contributions: Y.Z., Z.W., Y.X. and B.W. designed the study. Y.X. and G.L. established the animal models and collected tissue samples. Y.Z., Z.W., Y.X., P.Y. and Y.S. performed the experiments. J.P. and H.L. performed data analysis and drafted the manuscript. All authors contributed to the interpretation of the data, critically reviewed and edited the manuscript, and approved the version to be published.

Acknowledgments: The authors would like to thank all study participants and acknowledge the laboratory assistance from the Institute of Life Sciences, Youjiang Medical University for Nationalities, and the Life Science and Clinical Medicine Research Center, Affiliated Hospital of Youjiang Medical University for Nationalities.

Funding: This study was supported by the Key Project of the Guangxi Natural Science Foundation (No. 2023GXNSFDA026008), the Open Competition Project of the Guangxi Plateau Discipline (No. YY2026GYZ02), the 2026 Guangxi Master's Student Innovation Project (No. YCSW2026656), and the 2026 University-Level Graduate Student Innovation Program (No. YXCXJH2026010).

Conflicts of Interest: The authors declare that they have no conflicts of interest.

Ethics approval: Animal experiments were conducted in accordance with relevant guidelines and regulations(e.g. the revised Animals (Scientific Procedures) Act 1986 in UK and Directive 2010/63/EU in Europe). All animal experiments were approved by the Ethics Committee of Youjiang Medical University for Nationalities (approval Nos. 2024092503 and 2025040200).

Consent to participate: not applicable. No human participants or human data were involved in this study.

Consent for Publication: not applicable. No human participants or human data were involved in this

study.

References:

[1] American D A P P. 2. Diagnosis and Classification of Diabetes: Standards of Care in Diabetes-2026[J]. Diabetes care, 2026,49(Supplement_1):S27-S49.DOI:10.2337/dc26-S002.

[2] Genitsaridi I, Salpea P, Salim A, Sajjadi S F, Tomic D, James S, Thirunavukkarasu S, Issaka A, Chen L, Basit A, Luk A O Y, Ma R C W, Mbanya J, Ramachandran A, Wild S H, Duncan B B, Boyko E J, Magliano D J. 11th edition of the IDF Diabetes Atlas: global, regional, and national diabetes prevalence estimates for 2024 and projections for 2050[J]. The lancet. Diabetes & endocrinology, 2026,14(2):149-156.DOI:10.1016/S2213-8587(25)00299-2.

[3] Sun H, Saeedi P, Karuranga S, Pinkepank M, Ogurtsova K, Duncan B B, Stein C, Basit A, Chan J C N, Claude Mbanya J, Pavkov M E, Ramachandaran A, Wild S H, James S, Herman W H, Zhang P, Bommer C, Kuo S, Boyko E J, Magliano D J. Erratum to "IDF Diabetes Atlas: Global, regional and country-level diabetes prevalence estimates for 2021 and projections for 2045" [Diabetes Res. Clin. Pract. 183 (2022) 109119][J]. Diabetes research and clinical practice, 2023,204:110945.DOI:10.1016/j.diabres.2023.110945.

[4] Chen L, Sun S, Gao Y, Ran X. Global mortality of diabetic foot ulcer: A systematic review and meta-analysis of observational studies[J]. Diabetes, obesity & metabolism, 2023,25(1):36-45.DOI:10.1111/dom.14840.

[5] Zheng A, Ma H, Liu X, Huang Q, Li Z, Wang L, Zeng N, Wu B. Effects of Moist Exposed Burn Therapy and Ointment (MEBT/MEBO) on the autophagy mTOR signalling pathway in diabetic ulcer wounds[J]. Pharmaceutical biology, 2020,58(1):124-130.DOI:10.1080/13880209.2019.1711430.

[6] 向玥腴, 郑爱甜, 吴标良. 重塑糖代谢重编程抑制 M1 型巨噬细胞极化治疗糖尿病创面[J]. 2026,2026(2026-8-2).

[7] Zhang J, Hao L, Li S, He Y, Zhang Y, Li N, Hu X. mTOR/HIF-1α pathway-mediated glucose reprogramming and macrophage polarization by Sini decoction plus ginseng soup in ALF[J]. Phytomedicine : international journal of phytotherapy and phytopharmacology, 2025,137:156374.DOI:10.1016/j.phymed.2025.156374.

[8] Fendt S. 100 years of the Warburg effect: A cancer metabolism endeavor[J]. Cell, 2024,187(15):3824-3828.DOI:10.1016/j.cell.2024.06.026.

[9] Stegen S, Carmeliet G. Metabolic regulation of skeletal cell fate and function[J]. Nature reviews. Endocrinology, 2024,20(7):399-413.DOI:10.1038/s41574-024-00969-x.

[10] Li M, Dong Y, Shang Y, Liu J, Wang Y, Zhang D, Zhang L, Han C, Zhang Y, Shen K, Yang Y, Wang H, Guan H, Hu D. Metformin Syncs CeO(2) to Recover Intra- and Extra-Cellular ROS Homeostasis in Diabetic Wound Healing[J]. Small (Weinheim an der Bergstrasse, Germany), 2024,20(52):e2407802.DOI:10.1002/smll.202407802.

[11] Hou J, Chen L, Zhou M, Li J, Liu J, Fang H, Zeng Y, Sun J, Wang Z. Multi-Layered Polyamide/Collagen Scaffolds with Topical Sustained Release of N-Acetylcysteine for Promoting Wound Healing[J]. International journal of nanomedicine, 2020,15:1349-1361.DOI:10.2147/IJN.S232190.

[12] Louiselle A E, Niemiec S M, Zgheib C, Liechty K W. Macrophage polarization and diabetic wound healing[J]. Translational research : the journal of laboratory and clinical medicine,

2021,236:109-116.DOI:10.1016/j.trsl.2021.05.006.
[13] Damasceno L E A, Prado D S, Veras F P, Fonseca M M, Toller-Kawahisa J E, Rosa M H, Públio G A, Martins T V, Ramalho F S, Waisman A, Cunha F Q, Cunha T M, Alves-Filho J C. PKM2 promotes Th17 cell differentiation and autoimmune inflammation by fine-tuning STAT3 activation[J]. The Journal of experimental medicine, 2020,217(10):e20190613.DOI:10.1084/jem.20190613.
[14] Zheng D, Jiang Y, Qu C, Yuan H, Hu K, He L, Chen P, Li J, Tu M, Lin L, Chen H, Lin Z, Lin W, Fan J, Cheng G, Hong J. Pyruvate Kinase M2 Tetramerization Protects against Hepatic Stellate Cell Activation and Liver Fibrosis[J]. The American journal of pathology, 2020,190(11):2267-2281.DOI:10.1016/j.ajpath.2020.08.002.
[15] Campbell L, Saville C R, Murray P J, Cruickshank S M, Hardman M J. Local arginase 1 activity is required for cutaneous wound healing[J]. The Journal of investigative dermatology, 2013,133(10):2461-2470.DOI:10.1038/jid.2013.164.
[16] Willenborg S, Sanin D E, Jais A, Ding X, Ulas T, Nüchel J, Popović M, MacVicar T, Langer T, Schultze J L, Gerbaulet A, Roers A, Pearce E J, Brüning J C, Trifunovic A, Eming S A. Mitochondrial metabolism coordinates stage-specific repair processes in macrophages during wound healing[J]. Cell metabolism, 2021,33(12):2398-2414.DOI:10.1016/j.cmet.2021.10.004.
[17] Rovira-Llopis S, Bañuls C, Diaz-Morales N, Hernandez-Mijares A, Rocha M, Victor V M. Mitochondrial dynamics in type 2 diabetes: Pathophysiological implications[J]. Redox biology, 2017,11:637-645.DOI:10.1016/j.redox.2017.01.013.